

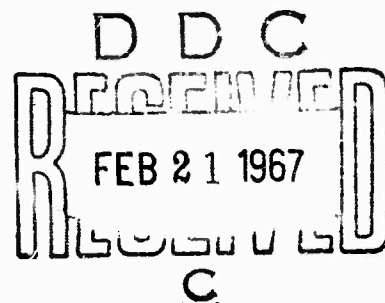
AD 647065

TECHNICAL SUMMARY REPORT  
TO  
ADVANCED RESEARCH PROJECTS AGENCY  
ON  
MATERIALS PREPARATION AND CHARACTERIZATION RESEARCH

For the period 1 July 1966 to 31 December 1966

Contract No. DA-49-083 OSA-3140

ARPA Order No. 338, Amendment 2



THE MATERIALS RESEARCH LABORATORY

THE PENNSYLVANIA STATE UNIVERSITY  
UNIVERSITY PARK, PENNSYLVANIA

ARCHIVE COPY

Technical Summary Report

To

ADVANCED RESEARCH PROJECTS AGENCY

On

Materials Preparation and Characterization Research

For the period July 1, 1966 to December 31, 1966

Contract No. DA-49-083 OSA-3140

ARPA Order No. 338, Amendment 2

Contract issued by:

Department of the Army

Defense Supply Service - Washington

Room 1D243, The Pentagon

Washington, D. C. 20310

Contract Amount: \$500,000

Contract Date: 10 February 1966

Expiration Date: 30 June 1967

Rustum Roy

The Pennsylvania State University

Telephone: 814-865-3421

Materials Research Laboratory

1-112 Research Unit No. 1

University Park, Pennsylvania 16802

## 1. INTRODUCTION:

### 1.1 Nature of Report

This report constitutes the third semi-annual technical report on this contract. It will be noted that the previous report was made in the nature of an annual report of the entire Materials Research Laboratory at The Pennsylvania State University, and included the work supported by the ARPA Contract as one part. It is planned to repeat that report format again in July 1967. For this half-yearly report, however, we present short summaries of the status of only those research programs supported directly from the present Contract.

### 1.2 Summary of Activities

In the crystal growth area some major studies have been finished up as Ph.D. dissertations and new lines of work are starting up. One of the new areas concerns the criteria determining the ability to prepare as non-crystalline phases materials which have never been so prepared before. Another is concerned with the preparation of "concentrated" solid solutions by a vapor deposition and subsequent controlled  $pO_2$  anneal. Still another is concerned with preparation of perovskite-family halides of the  $CsSnCl_3$  type.

In the area of characterization one major effort was the holding of the first International Conference on the Characterization of Materials in November 1966 on the Penn State Campus. This conference helped to focus the attention of an interdisciplinary group of materials scientists on the necessity and importance of the 'characterization' of a solid parallel to studies of its properties.

Research in this area encompasses many subjects. The laser ultramicroscopy has been applied to a study of a variety of real materials. The application of electron excited x-ray emission spectra to the determination of structural parameters of thin films on light metals has proved very useful. X-ray methods are applied to the study of polytypism of gel-grown crystals, to the determination of strain in theoretically dense polycrystalline aggregates and to dislocation contents of overgrowths on seeds. New work relating detailed crystal structural parameters to magnetic and optical properties has been started under Professor R. E. Newnham, who joined the faculty during this period.

## 2. RESEARCH RESULTS: MATERIAL PREPARATION

### 2.1 Growth of Large Crystals

#### 2.1.1 Flux Method

##### 2.1.1.1 Single Crystal Growth of $\text{VO}_2$ by Isothermal Flux Evaporation

(S. Aramaki, R. Roy)

This work has just been completed and the following is a summary of a paper describing the results:

At the International Conference on Crystal Growth, one of the authors reported on the general applicability of the technique of evaporation of a flux to the growth of refractory oxide crystals. During the same year, at least two other papers appeared reporting the use of the same method in general. In the paper by Roy, however, reasons were given for various special advantages of this method, among them: in the growth of crystals of a variable valence metal oxide. This paper reports the results on the application of the IFE methods to the growth of  $\text{VO}_2$ .

Using the most recent equilibrium diagram for the high oxygen end of the system V-O by Kachi and Roy, the IFE method has been applied without any flux other than the high oxygen melts. The largest crystal grown is 1.5 cm in circular section x 5-6 cm thick. The method consisted of holding a melt of initial  $\text{V}_2\text{O}_5$  composition at  $1215^\circ\text{C}$  in a flowing atmosphere of  $\text{pO}_2$  of  $10^{-3.8}$  for about 30-50 hours.

##### 2.1.1.2 Oxide Crystals Having the Corundum Structure

(D. M. Roy, R. E. Barks)

Results of this research have been presented in papers at four different professional meetings, one publication is in press, and the Ph.D. dissertation of Ronald E. Barks, "Flux Growth of Single Crystals  $\text{R}_2\text{O}_3$  Oxides with the Corundum Structure", was completed in June 1966. Experimental work was largely suspended with the departure of Mr. Barks in June, and present effort is involved with preparation of manuscripts for publication.

## 2.1.2 Hydrothermal Growth

### 2.1.2.1 Metastable Growth (of $RO_2$ Oxides)

(R. Roy, S. Theokritoff)

Current research is directed toward the novel goal of reproducible growth of a thermodynamically metastable phase. The study on the transport mechanism and growth of  $RO_2$  rutile-structure oxides ( $SnO_2$ ,  $TiO_2$  and  $GeO_2$ ) was completed with the Ph.D. dissertation of M. L. Harvill. Using these data as a base, attempts are being made to grow the hexagonal quartz structure  $GeO_2$  from low temperature hydrothermal solutions onto a  $SiO_2$ -quartz substrate. A wide variety of growth conditions is being investigated. Although we have not had any success as yet it is not possible to evaluate the potential for hydrothermal growth of metastable quartz- $GeO_2$  at this stage.

### 2.1.2.2 Phase Relations in Zinc Sulfide

(H. L. Barnes, S. D. Scott)

In the last report, the univariant nature of the sphalerite (sulfur rich)-wurtzite (sulfur deficient) phase change as a function of  $S_2$  fugacity and temperature was demonstrated by hydrothermal and dry gas experiments. Since then, the hydrothermal experiments in concentrated NaOH solutions have been extended to  $700^\circ C$ . Sphalerite reappears as the stable phase at about  $570^\circ C$  in 6.2m,  $600^\circ C$  in 10m, and  $700^\circ C$  in 15m NaOH solutions. Thus for a given NaOH solution there is a phase change from sphalerite to wurtzite and then back to sphalerite with increasing temperature. Coincidental with the reappearance of sphalerite at high temperatures is the occurrence of a second solid phase consisting of large (5 mm. long), clear, colorless, water-soluble, crystals. These crystals contain both sodium and zinc (qualitative emission spectroscopic analysis) and could not be identified by powder x-ray diffraction. Quantitative chemical analyses are in progress in an effort to fully characterize this apparently new compound.

The recurrence of sphalerite above  $600^\circ C$  is undoubtedly due to the interference of the unknown sodium-zinc compound. The activity of aqueous

Zn-complex in the NaOH solutions is lowered resulting in the precipitation of sulfur rich (zinc deficient) zinc sulfide which is sphalerite. This also means that any attempts to control zinc sulfide compositions within the stability field of the sodium-zinc compound will be unsuccessful.

The polytypic structure of  $3^4$  hydrothermally grown wurtzite crystals has been determined by single crystal precession methods. Both 6H and mixed layer 6H+4H polytypes have been reproducibly grown with a very sharp phase change at  $570^{\circ} \pm 4^{\circ}\text{C}$  at 7000 psi. The 6H polytype is consistently formed between the sphalerite-wurtzite transition and  $570^{\circ}\text{C}$  and the mixed layer 6H+4H polytype above  $570^{\circ}\text{C}$ . This polytypic phase change appears to be independent of NaOH concentration and only slightly dependent on total pressure. The reproducible sharp phase boundary indicates a possible genuine thermodynamic control on polytypism in wurtzite perhaps dependent upon  $\text{S}_2$  fugacity and temperature.

Excellent growth of sphalerite single crystals has been obtained in 5M  $\text{NH}_4\text{I}$  solutions at  $450\text{--}500^{\circ}\text{C}$ . Carbon is added to the charge to act as an oxygen buffer to prevent corrosion of the gold tubes. In runs in which no buffer was present, large (up to 2mm.) platy single crystals of gold were grown. In addition, the sphalerite crystals (also up to 2mm. diameter) had a distinct purple color. The purpose of the  $\text{NH}_4\text{I}$  experiments is to obtain ZnS crystal growth near neutral pH so that pyrrhotite ( $\text{Fe}_{1-x}\text{S}$ ) can be added as a  $\text{S}_2$  fugacity indicator. Eventually, large diameter gold tubes will be used to grow large sphalerite crystals in  $\text{NH}_4\text{I}$  solutions.

#### 2.1.2.3 Hydrothermal Growth of HgS Crystals

(H. L. Barnes, S. D. Scott)

In the last report, a method of growing mercury sulfide (cinnabar) crystals on a cold finger inserted into a rocking hydrothermal pressure vessel was described. The results of several runs in NaHS solutions are listed below:

Run	Molality NaHS	pH	Temperature, °C Solution Finger		Duration (days)	Results
M-11	3.7	8	150	27	7	Thick coating of lmm. long crystals.
M-12	3.7	8	70	26	12-1/2	Same as M-11
M-13	3.7	8	165	155	11	About the same as M-11 and M-12 but crystals somewhat smaller.
M-14	1.0	7	135	120	26	No crystal growth.

The pH's and temperature gradients were chosen on the basis of solubility data for HgS in NaOH-H<sub>2</sub>S-H<sub>2</sub>O solutions (Romberger et al., in preparation). In runs M-11, 12, and 13 a large yield was obtained but spontaneous nucleation prevented the growth of large single crystals. Since different temperature gradients had very little effect, an attempt was made in run M-14 to reduce the nucleation rate by lowering the solubility of HgS. At pH 7, HgS solubility is roughly proportional to the square of the bisulfide activity. Since no crystals were obtained in run M-14, it is apparent that the fourteen-fold reduction in HgS solubility was too severe.

The apparatus used in this research will not be available again until September, 1967. At that time, a seed technique will be used in an attempt to grow large single crystals.

#### 2.1.2.4 Growth of Hexagonal Selenium in High Pressure Liquid Ammonia

(J. F. Balascio, W. B. White, R. Roy)

This study has been completed and was successfully defended as the M.S. Thesis of J. F. Balascio. No further work on liquid ammonia growth is contemplated at the present time.

#### 2.1.2.5 Growth of Calcite

(J. F. Balascio, W. B. White, R. Roy)

The growth of optical quality calcite forms a peculiar paradox in materials preparation. Calcite crystals occur in nature in a wide variety

of environments but attempts spanning over two generations to grow calcite in the laboratory have met with little success. The object of this study, just begun in the past report period, will be to grow calcite from fluxes, flux-fluid mixtures, and from hydrothermal fluids. The hydrothermal equipment has been modified to use high carbon dioxide pressures and a controlled cooling control system has been installed. Initial attempts are being made to grow calcite from  $\text{Li}_2\text{CO}_3$  fluxes under moderate  $\text{CO}_2$  pressures.

### 2.1.3 Growth from Melt

#### 2.1.3.1 Bridgman Growth

(K. Vedam, W. B. White)

The Bridgman furnaces have been used to grow boules of InSb and with a special gas handling arrangement, to grow  $\text{LiF:GaF}_3$  and  $\text{LiF:FeF}_3$ .

#### 2.1.3.2 Growth of Crystals by Arc-Fusion

(L. Brown, W. B. White)

Fusion experiments with MgO have been continued with the hope of optimizing power flow and cooling program conditions. Several batches have produced usable crystals of MgO in the  $\text{cm}^3$  size range but more work remains to be done before the method is perfected.

A few runs have been made to grow CaO which is needed as a substrate material and to grow forsterite,  $\text{Mg}_2\text{SiO}_4$ , for elastic constant measurements. The forsterite also poses an interesting growth problem since the melt contains molecular entities and is more viscous than the completely ionic MgO and CaO melts. So far all material has been "micro-crystalline" and improved methods of inserting the feed material are being sought.

### 2.1.4 Traveling Solvent Method

#### 2.1.4.1 Growth of InSb-GaSb Solid Solutions

(R. W. Hamaker and W. B. White)

Single crystal regrowth of polycrystalline solid solutions has been accomplished using  $(\bar{1}\bar{1}\bar{1})$  oriented InSb seed substrates. Both In and Sb were utilized as zone metals\*. Figure 1 shows typical electron microprobe

---

\* Growth rates as large as several mm/week were observed at seed temperatures as high as  $450^\circ\text{C}$ .



MICROPROBE ANALYSES ALONG GROWTH DIRECTION IN  $Ga_x$ ,  $In_{1-x}$ , Sb

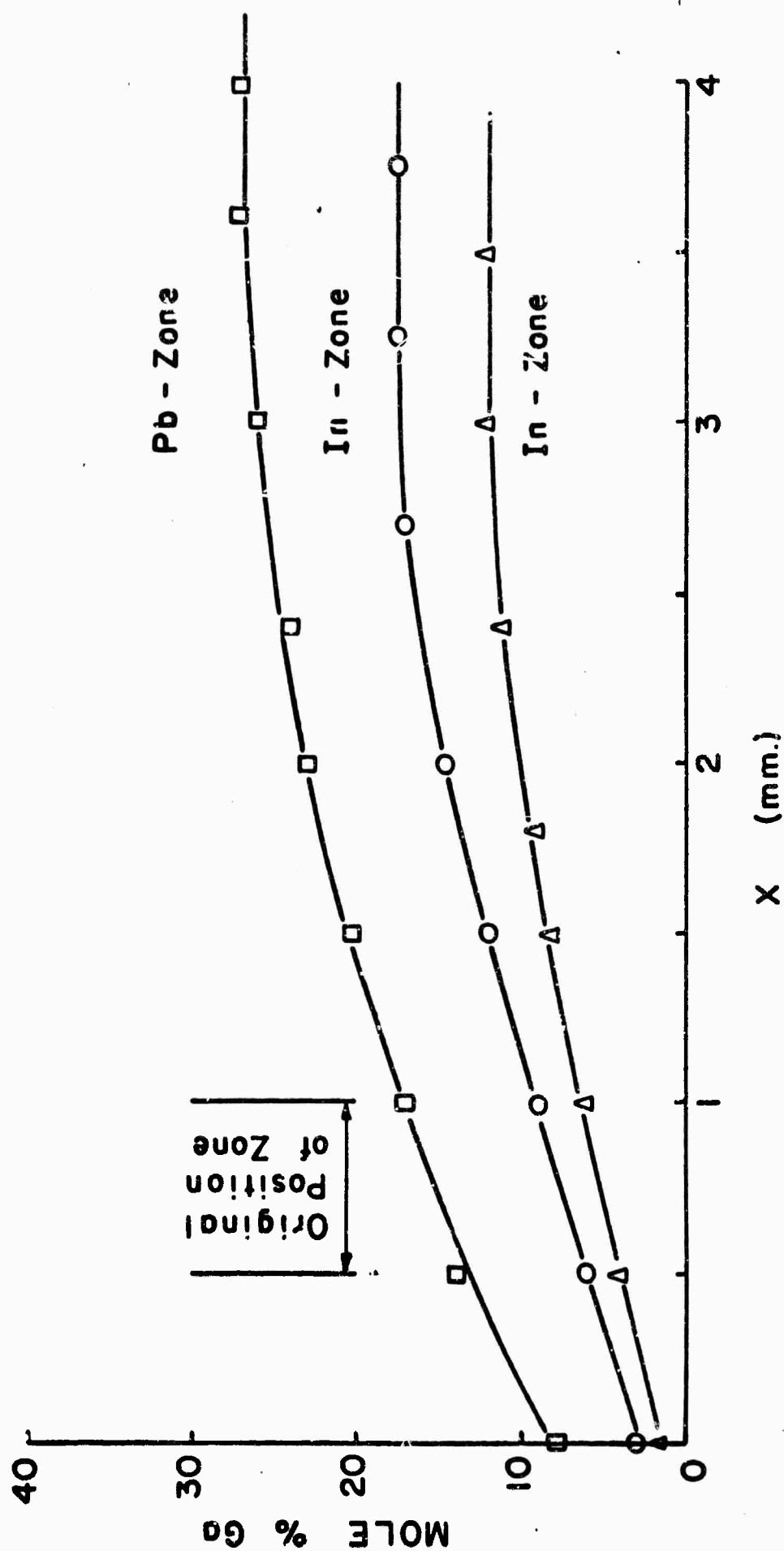


Figure 1. Microprobe Analyses Along Growth Direction in  $Ga_x$ ,  $In_{1-x}$ , Sb

analyses of compositional changes across the regrowth layers. Microprobe analyses on several samples having Pb as the zone metal have indicated no detectable Pb in the regrowth layers, corresponding to less than one part lead in approximately  $10^5$ .

Pressed InSb-GaSb powder samples were also used as feed material, but with no success. Uniaxial pressures up to 20 kbars were employed in making the pellets in an evacuated chamber (approximately 10 $\mu$  pressure) and heated to 200°C. In these runs erratic zone migration was evident. It is felt that grain boundary oxidation could have produced this anomalous migration behavior.

#### 2.1.4.2 Chalcogenide Growth

(R. W. Hamaker, W. B. White)

Preliminary work has been completed for the planned growth of several II-VI compounds by TSM. A high temperature, high vacuum growth chamber has been constructed for this work, having the capability for handling more than 100 amperes of current through water cooled electrodes.

Hot pressed ZnSe and ZnS have been obtained from the Eastman Kodak Company and will be utilized as feed material, while oriented single crystal sections having the wurtzite structure will be used as growth substrates.

#### 2.1.5 Vapor Growth

##### 2.1.5.1 Growth of Oxides by Halide Vapor Hydrolysis

(V. Caslavskaya, R. Roy)

Work on this subject has contained the following items:

- 1) The growth of some special NiO epitaxial single crystals for physical measurements in other laboratories.
- 2) A literature study of the thermodynamic properties of halides and sulphides of germanium, chromium, tin and manganese for the purpose of using these as starting materials for vapor growth of single crystals of oxides which have the rutile type structure.
- 3) Preparation of rutile substrates for the growth of the  $RO_2$  phases.

## 2.1.6 Nucleation Studies

### 2.1.6.1 Crystal Growth and Subsolidus Decomposition in the System PbS-PbTe

(M. S. Darrow, W. B. White, R. Roy)

Recent phase equilibrium studies\* have shown that a complete crystalline solution series between PbS and PbTe exists over a narrow temperature range between 800°C and 675°C. This work constituted attempts to grow crystals of varying S/Te content by Bridgman and traveling heater techniques. Growth of the solid solutions, however, is complicated by a subsolidus exsolution dome extending from 800°C at 30 mole% PbTe to within less than 10% of the end members at 400°C.

For the Bridgman runs, mixed powders of PbS and PbTe were melted in evacuated silica capsules, slowly lowered through the freezing zone, annealed between the solvus and solidus, and finally quenched. All boules shattered when the capsules were opened, but in some cases large pieces (2-3mm) were salvaged which appeared to be single crystals in Laue photographs, and electron probe analysis indicated they were homogeneous within the probe resolution limits.

In the traveling heater technique, high purity lead was placed in the bottom of the capsules beneath 3cm. of pressed pellets of the mixed powders. The capsules were lowered through an R.F. coil at a rate of about 0.5cm per hour with hot zone temperatures ranging from 400 to 700°C. The molten lead should move up through the pellets by taking the feed material into solution and redepositing it at the lower (cooler) end of the capsule. In all cases, the lead zone moved only about a third of the way through the pellets, and the recrystallized material was polycrystalline. Apparently, considerable experimentation with rate of pull and temperature control will be required to perfect this method of growth, but theoretically it appears more promising than the Bridgman technique.

---

\*M. S. Darrow, W. B. White, R. Roy. Phase Relations in the System PbS-PbTe, Trans. Met. Soc. AIME 236, 654-658 (1966).

The incentive for growing single crystals of these solid solutions was the opportunity to determine if spinodal decomposition could be observed in the subsolidus region of this system. Decomposition studies have been initiated using the large grain pieces from the Bridgman runs. Electron micrographs show a definite change in morphology for samples heat treated at temperatures between the solvus and estimated spinodal and below the spinodal as compared to those quenched from the one crystalline phase region. Considerable other morphological detail is observed. However, lack of published experimental work on subsolidus spinodal decomposition, as well as doubts concerning the reliability of the theoretical calculation of the spinodal temperatures, make more work necessary before conclusions can be drawn.

#### 2.1.6.2 Nucleation Studies in Network-Forming Liquids

(J. S. Berkes, W. B. White)

To facilitate the handling of nucleation kinetics data for the precipitation of NiO, the liquidus for the system  $\text{NiO-Na}_2\text{O} \cdot 0.2\text{B}_2\text{O}_3$ ,  $\text{NiO-K}_2\text{O} \cdot 0.2\text{B}_2\text{O}_3$  and  $\text{NiO-Rb}_2\text{O} \cdot 0.2\text{B}_2\text{O}_3$  were transformed into a functional form. For instance, for the system  $\text{NiO-Na}_2\text{B}_4\text{O}_7$  the equation

$$\ln N_{(\text{NiO})} = - \frac{14168.093}{RT} + 3.931$$

represents the liquidus from 740°C to 1200°C with a standard error of estimate  $S(N,T) = 0.001$  and with a maximum discrepancy with experiment of 0.005 (molar ratio).

A better fit was obtained using the function

$$N_{(\text{NiO})} = \exp. \frac{-\Delta H_f^* (\ln T_{\text{mp}} - \ln T)}{RT}$$

where  $T_{\text{mp}}$  = melting point of NiO (°K)

$T$  = temp (°K)

$R$  = gas constant

$\Delta H_f^*$  = experimentally determined function.

For  $740^\circ < T < 900^\circ\text{C}$   $\Delta H_f^* = + 7871.6$

$900^\circ < T < 1200^\circ\text{C}$   $\Delta H_f^* = - 4.588T + 13308.9$

By using this function to represent the liquidus, in the specified temperature intervals, the discrepancy between the calculated and experimentally determined values in  $N_{\text{NiO}}$  at no time exceeded 0.001 (molar ratio NiO). This provides much greater precision in the determination of these liquidus curves.

Only preliminary work has been carried out on the nucleation kinetics of NiO in these systems. The results obtained from replicas of fractured surfaces by the electron microscope have not been illuminating to date. The use of the laser ultramicroscope to detect submicroscopic particles seems to show some promise but no extensive data have yet been obtained.

#### System NiO-Li<sub>2</sub>O·2B<sub>2</sub>O<sub>3</sub>

In the pseudobinary system NiO-Li<sub>2</sub>O·2B<sub>2</sub>O<sub>3</sub> the liquidus separating the field of liquid and liquid + 3NiO·B<sub>2</sub>O<sub>3</sub> crystals has been determined accurately and single crystals of 3NiO·B<sub>2</sub>O<sub>3</sub> have been grown by the flux technique.

#### System NiO-B<sub>2</sub>O<sub>3</sub>

Only one binary compound (3NiO·B<sub>2</sub>O<sub>3</sub>) has been detected in the system NiO-B<sub>2</sub>O<sub>3</sub>. A two liquid region exists in the B<sub>2</sub>O<sub>3</sub> rich side of the system.

### 2.2 New Techniques

#### 2.2.1 Growth of Concentrated Crystalline Solutions: Rare Earth Vapor Deposition, Oxidation, and Subsequent High Temperature Diffusion Studies with MgO and TiO<sub>2</sub> Substrates

(L. E. Murr, R. Roy)

This study is concerned with attempts to vapor deposit thick, uniform layers of rare earth metals (Er, Tm) onto (100) oriented substrates of MgO and TiO<sub>2</sub>, to oxidize the rare earth vapor-grown surface film in controlled oxygen partial pressures, and finally to diffuse the metal oxide layers into the bulk of the substrate crystal to a volume percentage of >1% at high temperature.

A special ultra-high vacuum evaporation unit has been constructed which is basically a slightly modified version of a design utilized by

Murr\* to study the vapor-deposited structures of FCC metals as a function of background pressure. The completed ultra-high vacuum unit has routinely attained nominal pre-evaporation pressures of  $10^{-9}$  torr, following a 5-6 hr. bake of the ultra-high vacuum section, and without the necessity to cool the pumping and deposition chambers with liquid nitrogen. It is anticipated that the use of liquid nitrogen cooling in future work will provide routine pressures in the very low  $10^{-10}$  torr range.

Thin films of erbium (99.90%) have been vapor deposited onto cleaved (100) faces of NaCl crystals in order to calibrate the weight-thickness relationship for the condensed film layers. The optical absorption of the erbium films is also being investigated, and thin sections are being prepared for examination of their structural features by transmission and diffraction electron microscopy using the techniques of characterization previously outlined for vapor deposited FCC metal foils by Murr and Inman<sup>+</sup>.

It has been determined that erbium is easily evaporated onto NaCl at low pressures ( $<10^{-8}$  torr), and films of erbium ranging in thickness to 3000 Å have been condensed on MgO (100) crystal substrates at room temperature ( $\sim 25^{\circ}\text{C}$ ). It appears feasible to vapor deposit erbium thin films of thicknesses ranging to  $\sim 10$  microns on MgO or  $\text{TiO}_2$  at room temperature employing pre-evaporation background pressures  $<10^{-8}$  torr.

### 2.2.2 Crystal Growth in Gels

(H. K. Henisch, J. Dennis, A. Dugan)

The experimental work outlined in the last semi-annual report has been consolidated and a paper on "Nucleation and Growth of Crystals in Gels" has been completed. It has been accepted for publication in the Journal of the Electrical Society and is now in print. Besides the matters already referred to in the last report, it gives an account of reseeded experiments, as follows.

Once nucleated in a gel, crystals grow until they reach a constant size. It has already been shown that this size is determined by the progressive exhaustion of the reagents. Replenishment of at least one (the diffusing) reagent is a simple matter, but the removal of the waste

\*L. E. Murr, Brit. J. Appl. Phys. 15, 1511-1515 (1964).

<sup>+</sup>L. E. Murr and M. C. Inman, Phil. Mag. 14, 135-153 (1966).

products of the reaction is not. If, therefore, a crystal of larger size is required, it must be reseeded into another gel. This is done by first gelling a small amount of sodium metasilicate in a tube, resting the seed upon the gel surface thus formed and covering its first with additional sodium metasilicate solution and, after second gelling, with the diffusing reagent. In the course of transferring the crystal from one growth system to another, its surfaces are generally damaged and possibly contaminated, resulting in polycrystalline growth. To prevent this, the temperature is raised immediately after reseeded in order to dissolve a portion of the seed, as is usual in all seeding procedures. When the temperature is subsequently lowered, growth proceeds in the normal way until the reagents are once again exhausted. The process can then be repeated. In a series of steps it is thus possible to grow considerably larger crystals than can ordinarily be obtained in a single growth system. The method has not yet been widely applied, but the principle is illustrated below on the basis of calcium and copper tartrate. The table given below shows the weights of particular crystals after successive reseeded stages. With care, their high degree of optical perfection can be fully maintained throughout this procedure.

Weight of Calcium and Copper Tartrate Crystals  
Before and After Re-Seeding

Crystal	Weight in mg.				
	Initial	1st Seeding	2nd Seeding	3rd Seeding	4th Seeding
calcium tartrate	137.2	354.0	820.5	939.2	1104.0
	175.6	401.4	873.5	1083.1	1204.1
	139.4	347.0	685.4	803.1	952.3
copper tartrate	21.2	43.3	63.5	78.4	96.3
	18.7	37.8	69.6	84.4	101.1
	18.4	30.2	66.0	81.7	103.4

#### Characterization of Gel-Grown $\text{PbI}_2$

Of the many types of crystals grown in gels,  $\text{PbI}_2$  has been selected for special attention, because it has several interesting properties which are readily measurable. However, its fundamental band structure is still

not perfectly understood and to some extent the methods used to monitor its defect structure remain to be clarified.

A survey of the literature showed that the quoted low frequency dielectric constants ( $K'$ ) of  $\text{PbI}_2$  ranged from  $K' = 2.35$  to 113! The availability here of large single crystals of  $\text{PbI}_2$  with flat parallel faces offered an opportunity to make more accurate dielectric measurements. The results, showing the dependence of the dielectric constant upon frequency ( $10^2 - 10^5$  cps), temperature ( $120^\circ - 450^\circ\text{K}$ ), and light have recently been reported (Dielectric Properties and Index of  $\text{PbI}_2$  Single Crystals", J. Phys. Chem. Solids [in print]). The low frequency dielectric constant at  $300^\circ\text{K}$  is 6.21 with only a slight temperature dependence. Measurements of the index of refraction from  $0.5\mu - 15\mu$  were also carried out and found to differ considerably from previously accepted results. A comparison of dielectric constant and long wavelength index of refraction indicates that  $\text{PbI}_2$  is considered less ionic than previously proposed. The addition of Cr and Fe impurities (trace amounts) did not produce a measurable change in  $K'$ .

The study of the optical properties of  $\text{PbI}_2$  which were referred to in the last report has now been completed and is being submitted for publication ("Fundamental Optical Absorption and Photoconduction in  $\text{PbI}_2$  Single Crystals"). A temperature dependence of the absorption edge  $\sim 5250\text{\AA}$  indicates that the absorption tail ( $\vec{E}_1c$ ) obeys an expression of the form

$$\alpha = \alpha_0 \exp \left[ \frac{h\nu - E_0}{kT} \right]$$

where  $\alpha_0$ ,  $E_0$  are constants characteristic of the material,  $\alpha$  is the absorption coefficient and  $h\nu$  is the incident photon energy. The absorption edge is dichromatic with a splitting  $\sim 0.048\text{eV}$  at  $\alpha = \sim 80\text{cm}^{-1}$ . The photoconductive response peaks corresponding to the two edges have also been measured.

An absorption band at  $4.2\mu$  ( $0.29\text{eV}$ ) has been correlated with the dark current activation energy ( $\sim 0.28\text{eV}$ ) and is attributed to an acceptor level, tentatively explained in terms of a defect from stoichiometry. The density of centers associated with this band has been estimated to  $10^{15}/\text{cm}^3$ . The presence of Cr, Tl and Fe in trace amounts do not noticeably change the absorption spectrum in the region from  $0.5\mu$  to  $15\mu$ . The energy level of these defects may be  $< 0.083\text{eV}$  and so cannot be optically detected with the



available apparatus.

Current activities aim at establishing the basic photoelectric properties of  $\text{PbI}_2$  (sensitivity, response time, superlinearity, trapping range, mobility) and to detect changes due to dopants (Cr, Tl, Fe).

### 2.2.2 Plasma Synthesis

(F. J. Vastola, B. E. Knox)

A new graduate student began working on this project in September. The equipment has been moved into a new laboratory, reassembled and tested. The student has been trained and has successfully made many acetylene films. Silicon films are currently being made and epitaxial growth of silicon is planned.

## 3. RESEARCH RESULTS: MATERIALS CHARACTERIZATION

### 3.1 Application of the Electron Microprobe to the Characterization of Solids

(E. W. White)

#### 3.1.1 Improved Instrumentation

The new solid state X-ray readout system is now completely installed and in routine use. This system consists of Hamner (AEC Modular design) amplifiers, pulse height analyzers, ratemeters, timers, scalers, a data scanner and an ITT Model 33 Teletype. It can automatically read out the time plus the counts from three scalers or, when time printout is not needed, one can record the output of four scalers. The teletype gives both a punched tape and hard print record of the data.

#### 3.1.2 X-ray Spectral Shift Studies

The  $\text{AlK}_\beta$  emission band has been recorded for a number of aluminum oxides and hydroxides including alpha and gamma  $\text{Al}_2\text{O}_3$ , diaspore, boehmite, bayerite and gibbsite. By measuring the band shape, wavelength and intensity it is usually possible to determine which of the above phases is present in an unknown specimen. The difference between alpha and gamma  $\text{Al}_2\text{O}_3$  is particularly striking - contrary to literature reports that claim no difference in the emission band for these two polymorphs.

The emission band for the alpha phase is a distinct doublet and hence much broader than the band from gamma  $\text{Al}_2\text{O}_3$ . This marked difference in the X-ray emission band from the two polymorphs facilitates characterization of thin amorphous oxide layers such as anodized aluminum.

### 3.2 New Techniques for the Study of X-ray Absorption Fine Structure

(E. W. White, J. Hach)

A new method of obtaining X-ray absorption fine structure is currently being investigated. Samples are bombarded with electrons and the continuous X-rays produced are absorbed as they pass out of the sample. The absorption fine structure can be observed by measuring the X-ray spectrum at high resolution using a low take-off angle. Tests to date have been carried out by using the target areas of standard X-ray diffraction tubes as samples. For the 1-2 Å wavelength region accelerating voltages of 35-50 kV, and take-off angles of 7-10 degrees appear to produce optimum resolution. The Self Absorption Fine Structure (S.A.F.S.) method of obtaining spectra yields a resolution which compares favorably with that obtained by the standard thin film methods. In the immediate future a much more detailed study of the role played by radiation wavelength, take-off angle, acceleration voltage and mass absorption coefficients in determining the resolution and contrast observed in the spectra will be evaluated. By extending the study to different materials the value of the S.A.F.S. method as a tool for materials characterization will be determined.

### 3.3 Construction and Testing of Vacuum Curved Crystal Spectrometer

(E. W. White)

Construction of the curved crystal spectrometer is nearly completed. Assembly and testing of the major components and sub-assemblies are progressing satisfactorily and it is anticipated that the spectrometer will be put into routine use within a few weeks.

Salient features of the spectrometer include:

- 1) Provision for electron and X-ray excitation of samples.
- 2) Multi-position, water-cooled specimen holder that facilitates study of up to twelve samples without having to break vacuum.
- 3) Use of crystals of radius from four through eleven inches, making

it feasible to optimize intensity versus resolution as well as being able to select commercially manufactured crystals from a wide variety of sources such as the various electron probe manufacturers.

- 4) Take-off-angle variable from zero to 45 degrees for studies of special effects such as self-absorption fine structure.
- 5) Crystal motion controlled externally to vacuum via precision tangent screw arrangement.
- 6) Use of the turbomolecular pumping system will facilitate studies of oxygen and carbon spectra with maximum freedom from specimen surface contamination.

This spectrometer will add greatly to our current capability for X-ray spectra studies.

### 3.4 Characterization of Gel-Grown Crystals

#### 3.4.1 Polytypism in Gel-Grown $\text{PbI}_2$ Crystals

(V. Vand, J. Hanoka)

In the previous report, it was mentioned that the electron microprobe was to be used to explore the question of a screw dislocation mechanism of polytypism in gel-grown  $\text{PbI}_2$ . We now feel that the probe work has yielded very positive results.

In the course of attempting to optimize growth conditions, it was found that under certain conditions, a number of very small crystals ( $<1\text{mm}$ ) would always be found growing on the very bottom of the test tube, even if there were no crystals growing in the region immediately above them. These crystals had evidently grown on some foreign nuclei which were large enough to settle to the bottom of the gel. A rough calculation indicated that these foreign nuclei should be just visible with the optical microscope and this was confirmed subsequently. These crystals were then removed and it was attempted to identify these nuclei using the electron microprobe.

The probe did not reveal any foreign nucleus on the surface of these crystals. However, the microscope observations indicated that the nuclei might be in the center of the crystals, so the slicing technique described in the previous ARPA report was used to explore this possibility and see

if an interior slice contained the foreign nucleus. This proved to be exactly the case and the probe showed clearly that these nuclei contained silver and were in the center of the crystals. The presence of the silver was traced to the "Reagent Grade" lead acetate used to grow the crystals. X-ray fluorescence analysis showed that the lead acetate contained  $0.35 \pm 0.05\%$  silver.

It was then inferred that  $\text{PbI}_2$  grows epitaxially on a AgI crystal, as the system contains iodine, and AgI has similar lattice dimensions to polytype 2H of  $\text{PbI}_2$ . The theory which these results support has been termed the epitaxial theory of polytypism and is discussed along with the experimental results in a paper to be published in the February issue of Materials Research Bulletin (Epitaxial Theory of Polytypism: Observations on the Growth of  $\text{PbI}_2$  Crystals, by V. Vand and J. I. Hanoka).

### 3.5 Surface Studies on NaF and $\text{CaF}_2$ in Various Ambient Atmospheres

(S. R. Sashital, K. Vadam)

As has been reported in the earlier two reports the surface layers of lithium fluoride and sodium fluoride crystals get contaminated by the oxygen in the ambient atmosphere and this is reflected in the changes in their mechanical and optical properties. For example, bending experiments on LiF revealed that the maximum outer-fibre strain is decreased and an increase in the yield point is also noticed. Further, the etch pattern around microhardness indentations on LiF show a decrease in the dislocation glide length, indicating that the tetragonal distortion around the  $(\text{O}^{2-}-\text{F}^-)$  vacancy complexes blocks the motion of the dislocations.

Similar studies have been carried out on single crystals of NaF and  $\text{CaF}_2$  with various ambient atmosphere such as pure oxygen, nitrogen, xylene,  $\text{CCl}_4$  and atmosphere saturated with water vapor. The results obtained are in complete agreement with the hypothesis that the surfaces of alkali and alkaline earth fluorides get easily contaminated with oxygen and the oxygen is preferentially adsorbed and later chemisorbed at the sites of dislocation emergence.

### 3.6 Use of a Laser Ultramicroscope for Detection of Imperfections in Solids

(K. Vedam, V. Vand)

This work has continued to yield interesting new results on various solids - both crystalline and amorphous, thereby demonstrating clearly the power and capabilities of this extremely simple technique as a tool for characterization of materials. The experimental details of this technique will not be repeated here as it has already been described in detail in a recent paper on "Use of Laser as a Source of Light for Ultramicroscopy and Light Scattering by Imperfections in Crystals: Investigations of Imperfections in LiF, MgO and Ruby" - J. Appl. Phys. 37, 2551 (1966). In what follows, some of the recent results obtained on some crystals, hot-pressed materials (Kodak-IRTRAN materials) and glasses are summarized.

Figs. 1 - 3 represent the laser-ultramicroscopic patterns obtained from single crystals of ruby grown by the Verneuil technique, the hydrothermal technique and from the flux, respectively. It is seen from these figures that the quality of the Verneuil grown crystals are the worst and that the flux grown crystals appear to be the best, at least from a consideration of the defects observed. This indicates that the temperature at which the crystals are grown seems to play the dominant role in the perfection of the crystals - the lower the temperature the better the quality of the crystals. This is in agreement with the conclusion arrived at by Sahagian<sup>\*,+</sup> from a study of the dislocation density by the etch-pit technique on ruby and sapphire crystals grown by various techniques.

Fig. 4 shows two views of the interface between the seed crystal and the overgrown crystalline quartz in a typical sample grown by the hydrothermal technique. Recently a batch of high quality synthetic quartz crystals have been obtained from Sawyer Research Products, Inc., East Lake, Ohio. It is not possible to detect the interface in these latter

---

\* C. S. Sahagian: "Crystal Perfection of  $\alpha$ -Al<sub>2</sub>O<sub>3</sub> as a Function of Growth Method". Air Force Cambridge Research Laboratories publication No. AFCRL-66-659, September 1966, PSRP No. 268.

+ C. S. Sahagian: Private communication.

crystals with the naked eye. However these crystals are currently being examined by the laser ultramicroscopy technique.

A large boule of synthetic spinel  $\text{MgAl}_2\text{O}_4$  was also examined, but no defects could be detected by this technique even after a careful search. This was particularly surprising when it is realized that (1) these crystals were grown by the Verneuil technique and such crystals are usually highly imperfect and (2) it is well known that the starting material for growing synthetic spinel is far from stoichiometric  $\text{MgO} \cdot \text{Al}_2\text{O}_3$ . An explanation of this puzzling question comes from the expression for the intensity of the light scattered by defects in a host crystal given by

$$I_u = A (m^2 - 1) / (m^2 + 2)^2 V^2 (1 + \cos^2 \theta)^4$$

where  $m$  is the ratio of the refractive index of the defect to that of the host medium, and the other symbols have the usual significance<sup>\*\*</sup>. Since the refractive indices of  $\text{MgO}$ ,  $\text{Al}_2\text{O}_3$  and  $\text{MgAl}_2\text{O}_4$  are all nearly equal, the value of  $m$  is almost unity, and the scattered intensity is almost negligible. In other words we have here the situation, in which both the defect and the host medium have very nearly the same refractive index for the particular wavelength employed. And this low  $\Delta n$  imposes "serious" limitation on the sensitivity of this technique in such cases. However, one could profitably employ a different wavelength since it is very rare that the dispersion of the refractive indices of the defect and the host medium are also exactly alike.

A number of optical glasses have also been examined but no defects could be detected by this technique. However a neodymium glass laser material exhibited a few defects, as shown in Figure 5. Currently this glass is being examined with an electron microprobe to detect any possible concentration of neodymium at these defect sites.

A few hot pressed ceramics like Kodak IRTRAN materials which are quite clear to the naked eye were also examined and typical results obtained on hot-pressed  $\text{MgO}$  (IRTRAN-4) are shown in Figs. 6 and 7 respectively. One

---

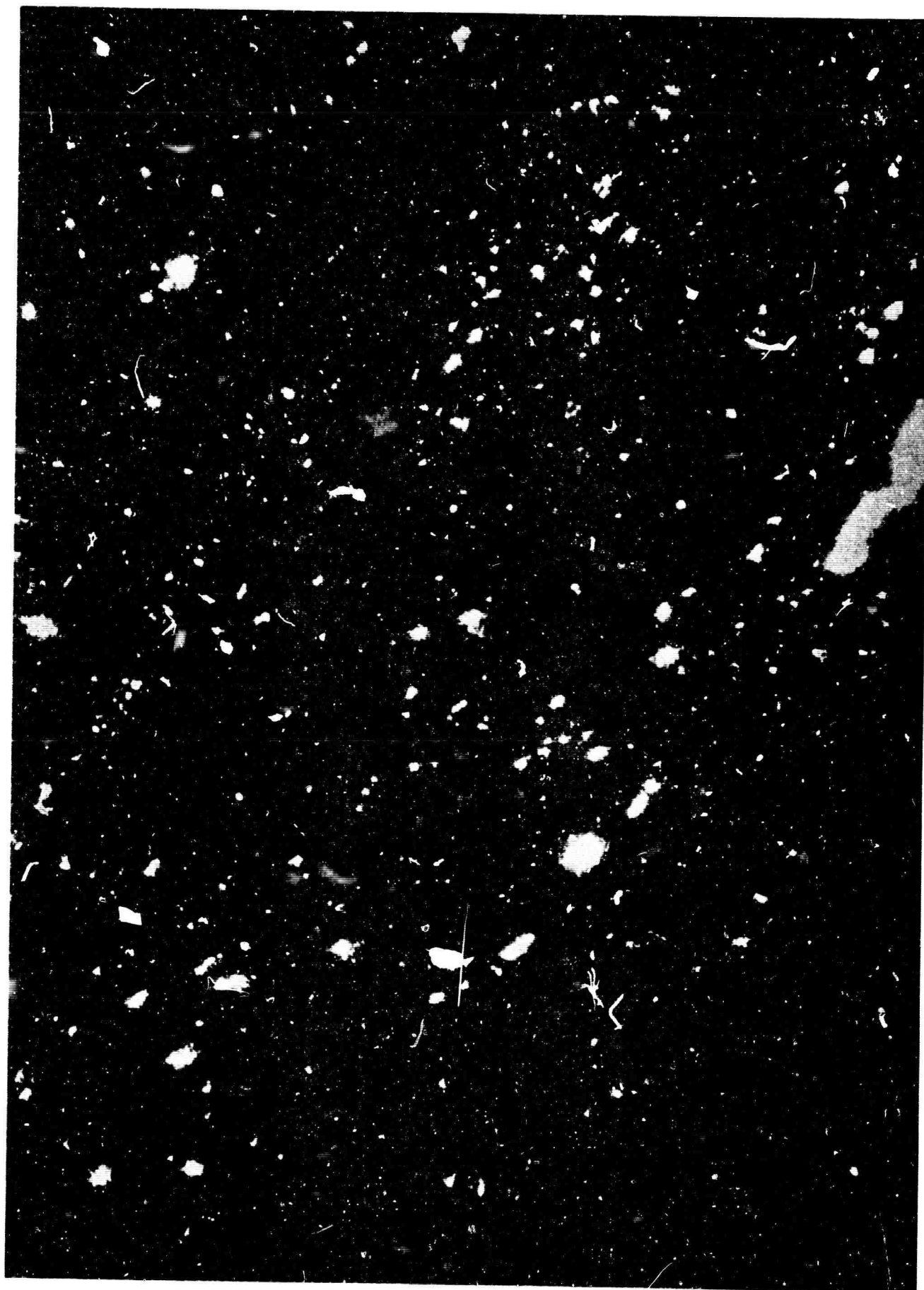
<sup>\*\*</sup> V. Vaná, K. Vedam and R. Stein, J. Appl. Phys. 37, 2551 (1966).



0.1 mm.

RUBY (FLAME FUSION)

Figure 1. Ruby (Flame Fusion)

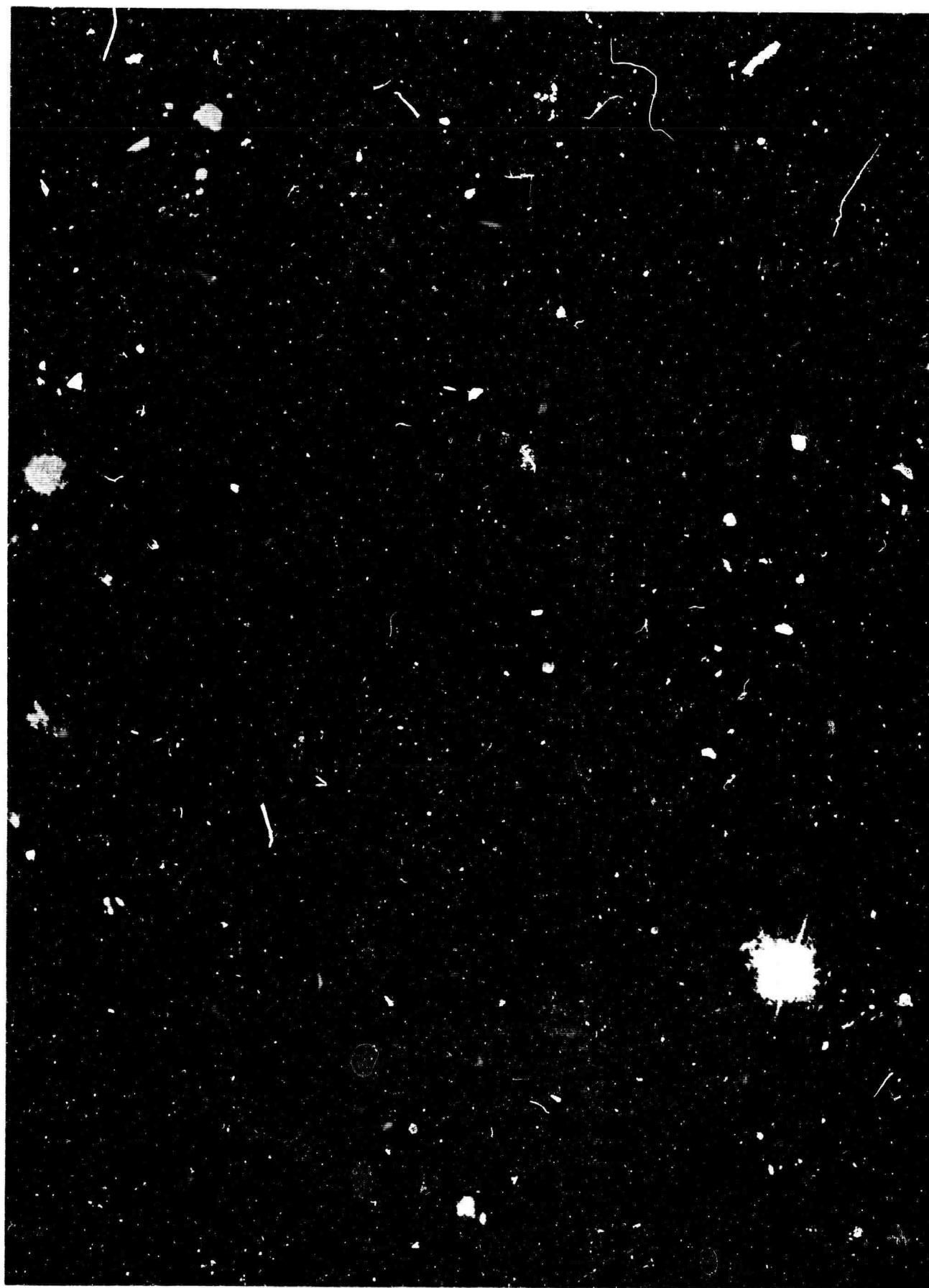


0.1 mm.

RUBY (HYDROTHERMAL)

Figure 2. Ruby (Hydrothermal)

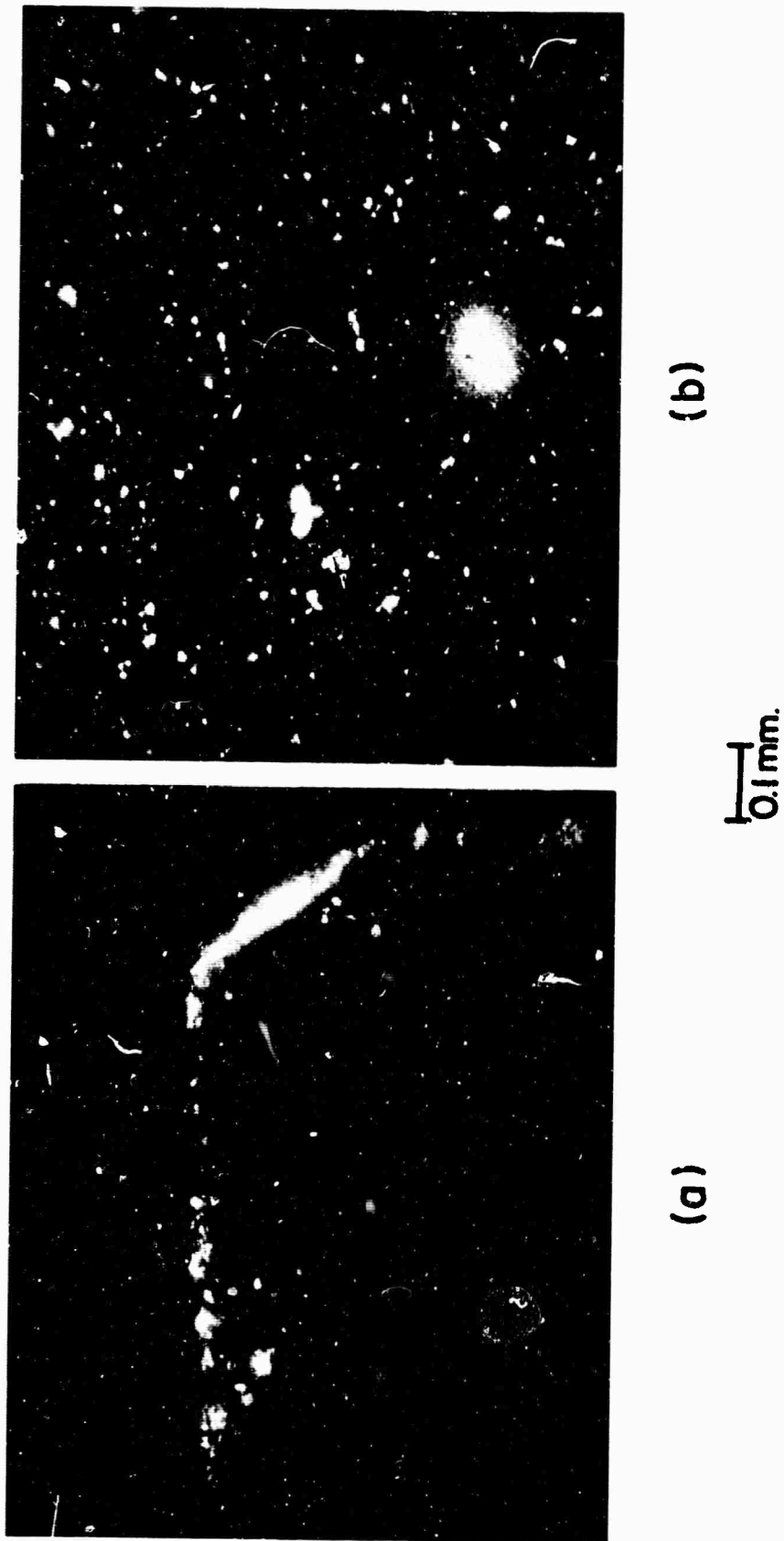




0.1 mm.

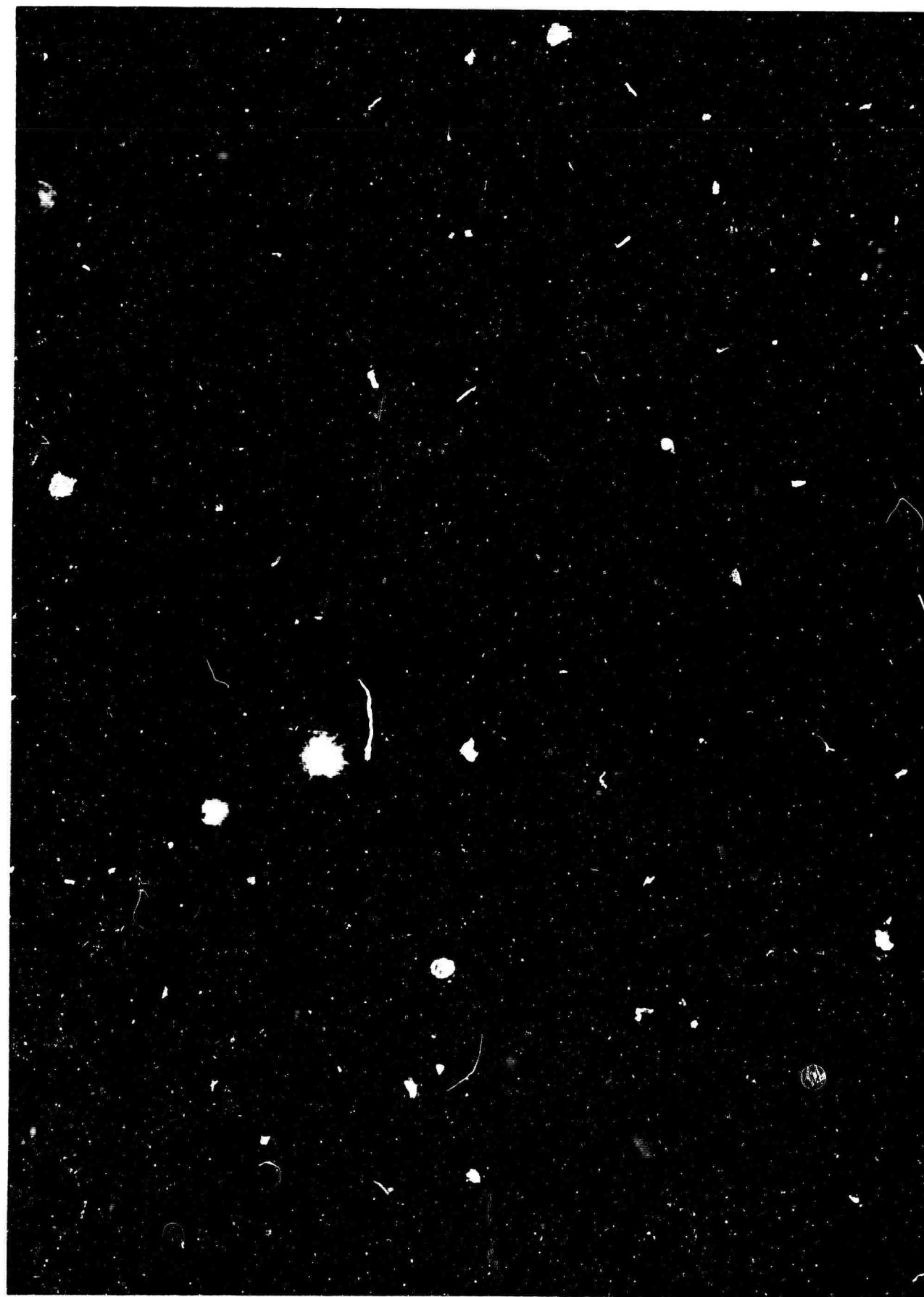
RUBY (FLUX GROWN)

Figure 3. Ruby (Flux Grown)



**SYNTHETIC QUARTZ (a) WITH SEED (b) INTERFACE  
BETWEEN THE SEED AND CRYSTAL**

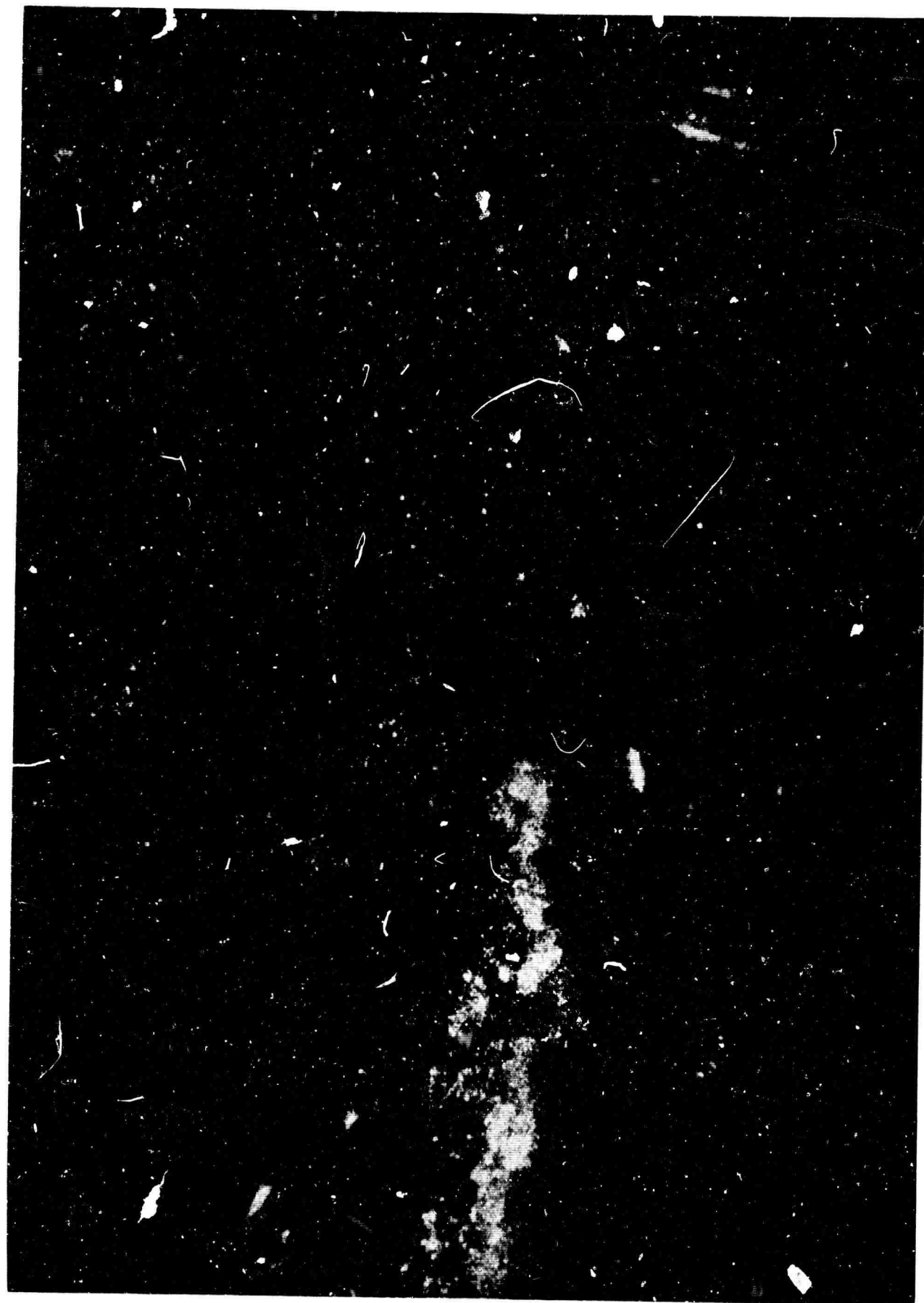
Figure 4. Synthetic Quartz (a) with Seed (b) Interface  
Between the Seed and Crystal



0.1 mm.

NEODYMIUM GLASS

Figure 5. Neodymium Glass



0.1mm.

HOT-PRESSED  $\text{CaF}_2$  (KODAK IRTRAN 3)

Figure 6. Hot-Pressed  $\text{CaF}_2$  (Kodak IRTRAN 3)

0.1 mm.

HOT-PRESSED MgO (KODAK IRTRAN 5)

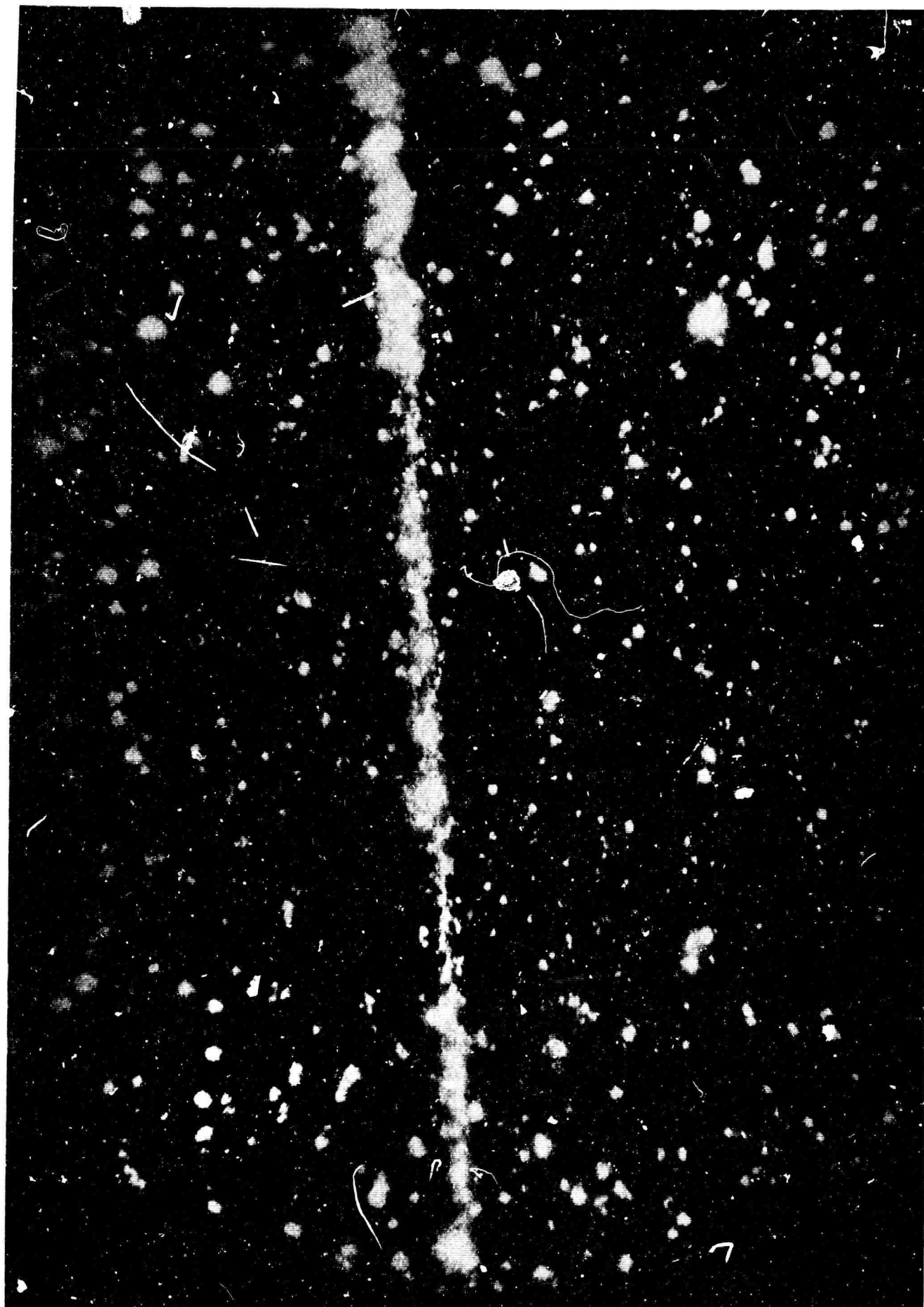


Figure 7. Hot-Pressed MgO (Kodak IRTRAN 5)

can easily recognize the grain boundaries and the concentration of defects at the grain boundaries and also the strands or regions of non-compacted material. This in spite of the fact that these materials will transmit coherent light and show no detectable dielectric evidence for the grain boundaries.

Some of these results formed the subject matter of a paper presented at the International Conference on Characterization of Materials held at this University during November 16-18, 1966. Currently efforts are under way (i) to increase the intensity of the laser light source by building a 100 mw He-Ne laser in order to improve the resolving power of the present unit and (ii) to convert the present laser to operate in the near infrared region in order to scan the interesting semiconductors like Si, GaAs, etc.

### 3.7 Characterization by X-ray Methods

#### 3.7.1 Strain in Hot-Pressed Magnesium Fluoride

(H. A. McKinstry, W. Stitt)

Attempts are being made to study by X-ray methods the residual strain in magnesium fluoride samples which are hot-pressed to theoretical density at 650°C and 30,000 psi. These new materials which constitute a new class of isotropized solids are taking on major significance as a new class of material. Small particle size can, of course, contribute to this broadening, but this type of broadening can be separated from the strain broadening using the Warren-Averbach method.

The 110, 220, 330, 101 and 303 peaks of hot-pressed magnesium fluoride were stepped-scanned at an interval of 0.02° in 2θ on a Picker X-ray diffractometer using CuKα radiation, and the intensities were automatically punched onto computer cards for processing. The sample was heated in stages to 650°C by means of a high temperature furnace; the data were obtained at five different temperatures, 25, 200, 400, 600 and 650°C. The data were analyzed by the Warren-Averbach method using a computer program which calculated the Fourier coefficients of each peak. This technique makes it possible to separate the peak broadening into strain and particle size contributions. The results of this analysis will be presented in the next report.

The line broadening of the original sample at 25°C was small and the width of the line decreased as the temperature was raised. At 650°C the

line width was assumed to be that of a strain-free material. The peak broadening can be described in a semi-quantitative way through the use of the expression  $(P-V)/P$  where  $P$  is the intensity of the  $K\alpha_1$  peak (minus background) and  $V$  is the intensity of the lowest point in the valley between  $\alpha_1$  and  $\alpha_2$ . The higher this value becomes, the better resolved is the peak and thus, the less the broadening. The table shows how this ratio increases with the temperature for  $MgF_2$ .

$T(^{\circ}C)$	$(P-V)/P$
25	.780
200	.80
400	.876
600	.886
650	.896
25 (after returning sample to room temperature)	.726

It is interesting to note that the broadening after the temperature studies is only slightly greater at room temperature than it was before heating. The sample became opaque and white after heating, an unexplained phenomenon well known in the industry.

### 3.7.2 Thermal Expansion of Hot-Pressed $MgF_2$

(H. A. McKinstry, W. Stitt)

In addition to the data required for the line broadening studies of the magnesium fluoride, sufficient high angle peaks were obtained for calculating lattice parameters as a function of temperature. The thermal expansion was then calculated in the range 0 to 650°C.

Only well resolved peaks with  $2\theta > 100$  degrees were used for the lattice parameter determination. The calculation of the parameters was done by computer using a least squares extrapolation against  $\cos^2\theta/\sin\theta$ . The expansion coefficients were then obtained by fitting a third degree polynomial to the lattice parameter data as a function of temperature.

Similar data were also taken for a powder which was crushed to 325 mesh from the hot-pressed sample.

The equations for the coefficients of expansion ( $\alpha = \frac{1}{a_0} \frac{da}{dT}$ ) of the hot-pressed  $\text{MgF}_2$  are,

$$\alpha_1 = 9.53 \times 10^{-6} + 1.56 \times 10^{-8}T - 1.40 \times 10^{-11}T^2$$

$$\alpha_3 = 13.1 \times 10^{-6} + 6.08 \times 10^{-9}T + 9.24 \times 10^{-12}T^2$$

where  $\alpha_1$  is in the direction parallel to a, and  $\alpha_3$  is parallel to c. Similarly the equations for the 325 mesh powder are,

$$\alpha_1 = 7.71 \times 10^{-6} + 2.57 \times 10^{-8}T - 2.53 \times 10^{-11}T^2$$

$$\alpha_3 = 11.1 \times 10^{-6} + 2.02 \times 10^{-8}T - 9.03 \times 10^{-12}T^2$$

These equations give the numerical values shown below.

T(°C)	Hot-pressed		325 mesh	
	$\alpha_1(\times 10^{-6})$	$\alpha_3(\times 10^{-6})$	$\alpha_1(\times 10^{-6})$	$\alpha_3(\times 10^{-6})$
25	9.9	13.3	8.3	11.6
200	12.1	14.7	11.8	14.8
400	13.6	17.1	13.9	17.8
600	13.9	20.1	14.0	20.0

If the  $\frac{c}{a}$  ratio is observed as a function of temperature, it is seen that  $\frac{c}{a}$  is approximately equal for the two samples at high temperatures, but the value for the hot-pressed sample becomes larger at lower temperatures than that of the powder.

The difference between the powder and hot-pressed materials at room temperature is also noticeable in the X-ray line width. The 325 mesh powder has a peak width which is essentially that of a strain-free sample, while the hot-pressed sample shows some peak broadening. Thus it seems that the appearance of strain in the hot-pressed material is accompanied by an increase in the  $\frac{c}{a}$  ratio.



### 3.7.3 Berg-Barrett Technique

(H. A. McKinstry, D. R. Lundy)

The Berg-Barrett camera is now available as a routine characterization tool. It is equipped with a Cu tube and spectroscopic film is used to record the images. Its major use is in the comparative perfection of crystals. For example, in growing a crystal from seeds, one can examine the seeds and later the crystal to see if there are any topographic features of the grown crystal derived from the seeds.

### 3.7.4 Powder Intensities as a Function of Temperature and Sample Preparation

(H. A. McKinstry, D. R. Lundy)

Since our last report some time has been spent in examining the effect of crystal perfection on the intensities of the x-ray diffraction peaks. It was noticed several years ago that after a sample was ground with a mortar and pestle the x-ray diffraction intensities at high angles were very considerably reduced. Upon annealing the intensities were markedly increased. This phenomena could be caused by one or a combination of factors such as 1) the mosaic character, 2) induced strains, 3) surface deformation, and 4) introduction of dislocations. One of the difficulties in assessing the effect of any of these factors is the experimental technique required to obtain reliable intensity measurements. The principal source of error apparently lies in the preparation of the sample. Several comparisons have been made using different techniques with the diffractometer. The precision of measurement for repeated measurements on one sample was within 2% for the great majority of peaks while the difference between different sample preparations was in excess of 20%. Reduction of particle size is expected to reduce the sample to sample differences which may then lead to data which can be analyzed quantitatively.

Since this problem is closely related to the standard temperature factor, speculations have been made as to whether atoms in a cubic material such as CsCl vibrate in a spherically symmetric way or whether it might be possible to describe their motion by a higher power polynomial, particularly in the neighborhood of the transition temperature. Preparations are being made to pursue this further.

### 3.8 Structure Analysis and Crystal Physics

(R. E. Newnham, J. F. Dorrian, J. P. Rarick)

Our research is devoted to the development of new materials with interesting magnetic, dielectric and optical properties. We have purposely avoided materials under intensive research elsewhere by concentrating on lesser known oxides. Succeeding paragraphs describe our most recent efforts.

A comprehensive study of magnetoelectric materials has been prepared. The magnetoelectric effect consists of two related phenomena: magnetization induced by an applied electric field and the inverse effect, polarization due to an external magnetic field. Magnetoelectricity was first suggested by Landau and Lifshitz in 1958 and verified experimentally a year later. Our report summarizes subsequent work through June 1966. Like many physical properties, the existence of magnetoelectricity depends on symmetry; the requisite elements were derived from thermodynamic arguments and several potential magnetoelectrics predicted. Among these are the  $\text{LiMPO}_4$  ( $M = \text{Ni, Co, Fe, Mn}$ ) compounds we investigated earlier.

The magnetic and optical properties of hydrous cupric silicate (diopase) have been measured.  $\text{CuSiO}_3 \cdot \text{H}_2\text{O}$  is a cyclosilicate containing  $\text{Si}_6\text{O}_{18}$  rings similar to beryl; the silicate rings are interconnected by copper atoms in square planar configuration. Cu-O-Cu exchange interactions lead to a surprisingly high Neel point of 70°K. Magnetic susceptibility data in the paramagnetic range give  $\theta = 70^\circ\text{K}$ ,  $\mu_{\text{eff}} = 1.86 \mu_B$ , and molecular field calculations predict a magnetic structure twice the size of the chemical unit cell. The diffuse reflectance spectrum of diopase is dominated by an intense absorption peak at  $13300 \text{ cm}^{-1}$ . Based on the approximate site symmetry  $C_{4v}$ , crystal field theory predicts a  $B_1 \rightarrow E$  electric-dipole transition in this wavelength range.

Polycrystalline zirconium titanate was investigated during a search for high temperature dielectric materials. Capacitance bridge measurements gave an average dielectric constant of  $K = 37$  in the 1Kc to 10Mc range. The crystal structure of  $\text{ZrTiO}_4$  was determined from x-ray diffractometer patterns and refined by least squares analysis. The space group is Pbcn, orthorhombic, with  $a = 4.81$ ,  $b = 5.45$ ,  $c = 5.03 \text{ \AA}$ ,  $Z = 2$ .

Titanium and zirconium are disordered in equipoint 4c (0, v, 1/4),  $v = 0.300 \pm 0.002$ , and oxygen is in general position 8d (x,y,z),  $x = 0.276 \pm 0.011$ ,  $y = 0.111 \pm 0.008$ ,  $z = 0.058 \pm 0.010$ . Oxygens form a distorted hexagonal close-packed array with metal ions occupying half the octahedral interstices. The mean (Zr,Ti)-O distance is  $2.04\text{\AA}$ .

The crystal structure and infrared spectrum of pollucite were investigated as a continuation of our study of trapped molecules in silicates. Pollucite single crystals with composition  $\text{Cs}_{.7}\text{Na}_{.3}\text{AlSi}_2\text{O}_6 \cdot 0.3\text{H}_2\text{O}$  contain water molecules trapped in aluminosilicate cages. A number of  $\text{H}_2\text{O}$  molecular vibration bands, similar to those of beryl and cordierite, are observed in the near infrared spectrum. The principal absorption band near  $2.7\mu$  is caused by the O-H stretching vibrations. This is accompanied by many smaller peaks at shorter wavelengths which are identified as combination bands involving the symmetric and unsymmetric stretching modes and the bending mode. The spectrum shows a marked similarity to that of water vapor. The crystal structure of pollucite has been refined by single-crystal x-ray analysis, beginning with the approximate structure proposed by Naray-Szabo. The space group is cubic,  $Ia\bar{3}d$ , with  $a = 13.682 \pm 0.003\text{\AA}$  and  $Z = 16$ . Ten least squares cycles based on 190 observed reflections gave an R-factor of 0.13 and the following coordinates:

$$\text{Cs in } 16b \left(\frac{1}{8}, \frac{1}{8}, \frac{1}{8}\right), B = 1.7 \pm 0.2.$$

$$(\text{Al}, \text{Si}) \text{ in } 48g \left(\frac{1}{8}, u, \frac{1}{4} - u\right), u = 0.6331 \pm 0.0009, B = 0.3 \pm 0.2.$$

$$\text{O in } 96h (x,y,z), x = 0.1036 \pm 0.0012, y = 0.1333 \pm 0.0014, z = 0.7216 \pm 0.0013,$$

$$B = 1.8 \pm 0.4.$$

From intensity calculations and crystallo-chemical arguments, we conclude that  $\text{Na}^+$  and  $\text{H}_2\text{O}$  substitute jointly for  $\text{Cs}^+$  in the large interstice, rather than the analcite arrangement. The mean (Si,Al)-O and Cs-O bond lengths are  $1.64$  and  $3.48\text{\AA}$ , respectively.

Two other problems are currently in progress. We are attempting to synthesize  $\text{CsSnCl}_3$  and related halogenides. Hopefully these are model structures of  $\text{BaTiO}_3$  and may exhibit useful ferroelectric phenomena. By incorporating divalent tin in the octahedral site, we intend to promote

$p^3$  covalent bonding, leading to trigonal distortion and spontaneous polarization along the body diagonal. Crystal growth is being attempted from the melt beginning with CsCl and  $\text{SnCl}_2$ . Powder patterns taken on preliminary runs give some indication of a perovskite phase. The second project concerns the magnetic properties of transition-metal tellurates. Ceramic specimens of  $\text{Fe}_2\text{TeO}_6$  and  $\text{Cr}_2\text{TeO}_6$  have been prepared and found to crystallize with the tri-rutile structure. Magnetic susceptibility and neutron diffraction studies will follow.

#### PUBLICATIONS, REPORTS, THESES

Two students completed their research for advanced degrees during this period:

J. Balascio, M.S. in Solid State Technology. Title of thesis:

"Crystal Growth in Liquid Ammonia."

J. Dennis, Ph.D. in Solid State Technology. Title of thesis:

"Crystal Growth in Gels." (All requirements met, degree not yet awarded).

M. L. Harvill, Ph.D. in Solid State Technology. Title of thesis:

"Hydrothermal Crystal Growth of the Rutile Structure Oxides:  $\text{TiO}_2$ ,  $\text{GeO}_2$  and  $\text{SnO}_2$ ."

The following papers were presented at meetings:

Barks, R. E. and Roy, Della M. Single crystal growth of  $\text{R}_2\text{O}_3$  (corundum structure) oxides by the flux method. Intl. Conf. on Crystal Growth, Boston, Mass., June 24 (1966).

Barnes, H. L. and Scott, S. D. Stoichiometry of sulfide minerals. Annual Meeting of Geol. Soc. America, San Francisco, Nov. (1966).

Henisch, H. K. Crystal growth in gels. Solid State Seminar sponsored by Minneapolis-Honeywell, Inc., Oct. (1966).

Newnham, R. E. and Santoro, R. P. Antiferromagnetism in  $\text{LiFePO}_4$ . Am. Phys. Soc. Meeting, Providence, R. I. (1966).

Newnham, R. E. and Farrell, E. F. Electronic and vibrational absorption spectra in cordierite. Intl. Conf. on Characterization of Materials, The Pennsylvania State University, University Park, Pa., Nov. 16-18 (1966).

- Vand, V. and Vedam. K. Use of a laser ultramicroscope for detection of imperfections in crystals. Intl. Conf. on Characterization of Materials, The Pennsylvania State University, University Park, Pa., Nov. 16-18 (1966).
- White, E. W. and Roy, R. Crystal chemical characterization of insulator solids by x-ray emission spectroscopy. Intl. Conf. on the Characterization of Materials, The Pennsylvania State University, University Park, Pa., Nov. 16-18 (1966).
- The following papers were published during this period:
- J. S. Berkes and W. B. White, "The Optical Spectra of Nickel in Alkali Tetraborate Glasses", Phys. Chem. Glasses (in press).
- J. Dennis and H. K. Henisch, "Nucleation and Growth of Crystals in Gels", J. Electrochem. Soc. (in press).
- A. Dugan and H. K. Henisch, "Dielectric Properties and Index of Refraction of  $\text{PbI}_2$  Single Crystals", J. Phys. Chem. Solids (in press).
- R. E. Newnham, L. G. Caron and R. P. Santoro, "Magnetic Properties of  $\text{CaCoSiO}_4$  and  $\text{CaFeSiO}_4$ ", J. Am. Ceram. Soc. 49:284-285 (1966).
- \_\_\_\_\_, R. P. Santoro, P. F. Seal and G. R. Stollings, "Antiferromagnetism in  $\text{Mn}_3\text{B}_2\text{O}_6$ ,  $\text{Co}_3\text{B}_2\text{O}_6$  and  $\text{Ni}_3\text{B}_2\text{O}_6$ ", Phys. Stat. Solidi 16: K17-K19 (1966). (Work done at M.I.T.).
- \_\_\_\_\_, E. F. Farrell, "Electronic and Vibrational Absorption Spectra in Cordierite", Am. Mineral. (in press) (Work done at M.I.T.).
- \_\_\_\_\_, R. P. Santoro, "Magnetic and Optical Properties of Diopside", Phys. Stat. Solidi (in press).
- R. E. Newnham, "Crystal Structure of  $\text{ZrTiO}_4$ ", J. Am. Ceram. Soc. (in press).
- \_\_\_\_\_, "Crystal Structure and Optical Properties of Pollucite", Am. Mineral. (submitted).
- L. B. Robinson, W. B. White and Rustum Roy, "Growth of Transition Metal Oxide Crystals by Halide Vapor Hydrolysis", J. Mat. Sci. 1:336-345 (1966).
- Rustum Roy, "Application of the Isothermal Flux Evaporation Method", Mat. Res. Bull. 1:299 (1966).

- R. P. Santoro, R. E. Newnham and S. Nomura, "Magnetic Properties of  $\text{Mn}_2\text{SiO}_4$  and  $\text{Fe}_2\text{SiO}_4$ ", J. Phys. Chem. Solids 27:655-666 (1966).  
(Work done at M.I.T.).
- \_\_\_\_\_, D. J. Segal and R. E. Newnham, "Magnetic Properties of  $\text{LiCoPO}_4$  and  $\text{LiNiPO}_4$ ", J. Phys. Chem. Solids 27:1192-1193 (1966).  
(Work done at M.I.T.).
- \_\_\_\_\_, R. E. Newnham, "Survey of Magnetoelectric Materials",  
Tech. Report AFML-TR-66-327, 24 pp., Sept. (1966). (Work done at M.I.T.).
- \_\_\_\_\_, R. E. Newnham, "Antiferromagnetism in  $\text{LiFePO}_4$ ", Acta Cryst.  
(in press). (Work done at M.I.T.).
- D. J. Segal, R. P. Santoro and R. E. Newnham, "Neutron-Diffraction Study of  $\text{Bi}_4\text{Si}_3\text{O}_{12}$ ", Z. Krist. 123:73-76 (1966). (Work done at M.I.T.).
- V. Vand, K. Vedam and R. Stine, "The Laser as a Light Source for Ultra-Microscopy and Light Scattering by Imperfections in Crystals: Investigation of Imperfections in LiF, MgO, and Ruby", J. Appl. Phys. 37:2551 (1966).
- E. W. White and H. A. McKinstry, "Chemical Effect on X-ray Absorption-Edge Fine Structure", Advances in X-ray Analysis, Plenum Press, Vol. 9:376-392 (1966).

### PERSONNEL

We have added to the faculty since the Fall Term 1960, Dr. R. E. Newnham, Associate Professor of Solid State Science, formerly of the Electrical Engineering Department at M.I.T. All other faculty noted in the last report continue to be active in this program.

### FUTURE PLANS

Another addition to the faculty with major responsibility in this area will be made effective February 1, 1967, when Dr. J. W. Faust of the Westinghouse Electric Corporation, joins the staff as Professor of Solid State Science.

Various aspects of our work related to non-crystalline solids will be emphasized as the new cooperative program is phased in.